EUROPEAN ORGANIZATION FOR NUCLEAR RESEARCH

CERN-EP-2000-018
January 24, 2000

Search for Charginos with a Small Mass Difference to the Lightest Supersymmetric Particle at $\sqrt{s} = 189$ GeV

The L3 Collaboration

Abstract

A search for charginos nearly mass-degenerate with the lightest supersymmetric particle is performed using the 176 pb^{-1} of data collected at 189 GeV in 1998 with the L3 detector. Mass differences between the chargino and the lightest supersymmetric particle below 4 GeV are considered. The presence of a high transverse momentum photon is required to single out the signal from the photon-photon interaction background. No evidence for charginos is found and upper limits on the cross section for chargino pair production are set. For the first time, in the case of heavy scalar leptons, chargino mass limits are obtained for any $\tilde{\chi}_1^{\pm} - \tilde{\chi}_1^0$ mass difference.

Submitted to *Phys. Lett. B*

1 Introduction

Supersymmetry (SUSY) is one of the most appealing extensions of the Standard Model. In SUSY theories with minimal particle content (MSSM) [1], in addition to the ordinary particles, there is a supersymmetric spectrum of particles with spins which differ by one half with respect to their Standard Model partners.

Charginos ($\tilde{\chi}_1^{\pm}$), which are a mixture of the supersymmetric partners of $W^{\pm}$ (gaugino state) and $H^{\pm}$ (higgsino state), are pair produced via s-channel γ/Z exchange. The production cross section can be reduced by an order of magnitude when the t-channel scalar neutrino ($\tilde{\nu}$) exchange is important.

In this paper the hypothesis of R-parity conservation is made. The R-parity is a quantum number which distinguishes ordinary particles from supersymmetric particles. If R-parity is conserved supersymmetric particles are pair-produced and their decay chain always contains, besides standard particles, two Lightest Supersymmetric Particles (LSP). The LSP, which is stable and weakly-interacting, escapes detection. The LSP can be the lightest neutralino ($\tilde{\chi}_1^0$), a mixture of the supersymmetric partners of Z, γ, and neutral Higgs bosons, or the scalar neutrino.

As long as charginos are sufficiently heavier than the LSP, their decay products can be detected with high trigger and selection efficiencies. When the mass difference ($\Delta M = M_{\tilde{\chi}_1^{\pm}} - M_{\tilde{\chi}_1^0}$) is smaller than 4 GeV, the search described in Ref. [2] (hereafter referred as standard) becomes very inefficient, because in that range the signal and the photon-photon interaction background are indistinguishable.

For ΔM between a few hundred MeV and a few GeV, charginos decay near the interaction vertex and the energy carried by the visible decay products is so small that trigger inefficiencies become substantial. In addition, such a signal is overwhelmed by the photon-photon interaction background, which is rapidly increasing for decreasing masses of the photon-photon system. The trigger efficiency and the signal to background ratio can be improved by requiring in the event an Initial State Radiation (ISR) photon with high transverse momentum. Therefore, in this paper we report a search for the process

$$e^+e^- \;\rightarrow\; \gamma\tilde{\chi}_1^+\tilde{\chi}_1^- \;\rightarrow\; \gamma\tilde{\chi}_1^0\tilde{\chi}_1^0 X$$

where X stands for low energy standard charged particles.

This method was previously used in the Mark II experiment [3] in the search for a fourth lepton doublet, whose members are close in mass. It was then suggested [4] for the search at LEP for charginos nearly mass-degenerate with the LSP. The DELPHI collaboration recently published such a search in a data sample collected at $\sqrt{s} \leq 183$ GeV [5].

2 Data Sample and Monte Carlo Simulations

This search uses the data collected at 189 GeV with the L3 detector [6] for an integrated luminosity of 176 pb^{-1} . The following background processes are simulated: $e^+e^- \rightarrow \tau^+\tau^-\gamma(\gamma)$, $e^+e^- \rightarrow \mu^+\mu^-\gamma(\gamma)$ and $e^+e^- \rightarrow \nu\bar{\nu}\gamma(\gamma)$ with `KORALZ` [7], $e^+e^- \rightarrow W^+W^-\gamma(\gamma)$ with `KORALW` [8] and radiative Bhabha scattering with `TEEGG` [9]. The statistics of the Monte Carlo is equivalent to more than 60 times the integrated luminosity except for radiative Bhabha events where it is more than 16 times.

Photon-photon interactions with hadronic final state ($e^+e^- \rightarrow e^+e^-q\bar{q}$) can not be reliably simulated in the range of interest of this analysis, because of the large theoretical uncertainties

on the differential cross section in the non-perturbative regime. For photon-photon interactions with leptonic final states ($e^+e^- \to e^+e^-\ell^+\ell^-\gamma(\gamma)$) there is no complete Monte Carlo including the simulation of initial state radiation. For this reason, no photon-photon background is used.

Signal events are simulated with `SUSYGEN` [10] for chargino masses between 45 GeV and 88 GeV and ΔM from 30 MeV to 4 GeV. Only events with a photon more than 10° away from the beam pipe and with an energy greater than 4 GeV are considered. These requirements will be referred as fiducial cuts. The chargino decay branching ratios as in Ref. [4] are used. For ΔM smaller than 200 MeV, $\tilde{\chi}_1^\pm$ decay lengths of a few centimetres may occur. In this case, $\tilde{\chi}_1^\pm$ decays are treated by the `GEANT` [11] package.

The detector response is simulated using the `GEANT` package. It takes into account effects of energy loss, multiple scattering and showering in the detector materials and in the beam pipe. Hadronic interactions are simulated with the `GHEISHA` program [12]. Time dependent inefficiencies of the different subdetectors and of the trigger are also taken into account in the simulation procedure.

3 Low ΔM phenomenology

The search for low ΔM charginos accompanied by ISR photons does not suffer from the large photon-photon interaction background if the transverse momentum of the photon is large enough. While in signal events the missing momentum is due to weakly interacting particles, in photon-photon interactions it is due to the electrons escaping in the beam pipe. In the latter case, if a high transverse momentum photon is present the two final state electrons must be deflected into the detector. To suppress the photon-photon interactions, the following requirement on the photon transverse momentum is applied:

$$E_{T\gamma} \geq 2E_{\rm beam}\frac{\sin\theta_d}{1+\sin\theta_d} \tag{1}$$

where θ_d is the minimum detection angle for the deflected electron and $E_{\rm beam}$ is the beam energy. For the L3 detector, $\theta_d = 1.7°$ resulting in $E_{T\gamma} \geq 5.45$ GeV. With this requirement the photon energy is large enough to trigger the detector.

The ISR energy spectrum in signal events, as shown in Figure 1, depends on the relative contribution of the s-channel Z exchange, which in turn depends on the $Z\tilde{\chi}_1^\pm\tilde{\chi}_1^\pm$ coupling. A softer photon spectrum is expected in the case of higgsino-like charginos than in the case of gaugino-like charginos. In addition, when scalar neutrinos are as light as charginos the t-channel diagram becomes important and modifies the shape of the ISR energy spectrum as shown in Figure 1.

Chargino decay branching ratios in the low ΔM region change according to the opening of the various decay channels. For $\Delta M < 1.5$ GeV, the hadronic decay channel in one or two pions is enhanced and the decay spectrum is more similar to $\tau^\pm$ decays than to $W^\pm$ decays.

The $\tilde{\chi}_1^\pm$ decay length increases with decreasing ΔM. For $\Delta M \gtrsim 300$ MeV, the $\tilde{\chi}_1^\pm$ decays near the interaction vertex within 1 cm. For $m_{\pi^\pm} < \Delta M \lesssim 300$ MeV, the $\tilde{\chi}_1^\pm$ decays often inside the detector but a few centimetres away from the interaction vertex. For ΔM less than the $\pi^\pm$ mass, the $\tilde{\chi}_1^\pm$ decays outside the detector and appears as a heavy stable charged particle.

Chargino decays via virtual scalar lepton exchange occur if scalar leptons are as light as charginos, but only for gaugino-like charginos whose coupling to scalar leptons is strong enough. In general, the chargino width is not affected by supersymmetric scalar particles as long as they

are more than 15 GeV heavier than the $\tilde{\chi}_1^{\pm}$. The same is true for chargino branching ratios if supersymmetric scalar particles are at least 30 GeV heavier than the $\tilde{\chi}_1^{\pm}$.

As an example, chargino decays are purely leptonic and the chargino decay length is extremely short when the $\tilde{\nu}$ is mass degenerate with or lighter than the chargino. In the latter case, where the two-body decay channel $\tilde{\nu}_e e^{\pm}$ is open, chargino decay lengths are smaller than 1 cm as long as ΔM is more than the electron mass.

4 Analysis

4.1 Preselection

This preselection, as well as the following selections, are tailored only on the expected signal distributions, because, as mentioned in Section 2, the simulation of Standard Model background processes is incomplete.

The aim of the preselection is to keep events with at least two charged particles not necessarily coming from the interaction vertex and an energetic photon. The analysis relies mainly on the photon identification in the electromagnetic calorimeter (BGO). In addition, we use the tracking chamber to detect charged particles and to measure their momentum and eventually decay length. Additional energy deposits due to the soft chargino decay products are allowed, but no strict requirement is applied on them.

The BGO must contain an electromagnetic energy deposit more than 20° away from the beam pipe and with a transverse momentum compatible with equation (1). There must be no track in a 1° sector in the $r-\phi$ plane around the photon with a number of hits higher than 10 out of a maximum of 62. This photon has also to be isolated in space: neither a track with more than 10 hits nor a significant energy deposit in the BGO should be in a 15° cone around the photon. We also require that the event contains at least 2 tracks: one with at least 10 hits and a distance to the interaction vertex in the $r-\phi$ plane (DCA) smaller than 1 cm; and a second track satisfying either these criteria or having at least 20 hits. For signal events satisfying these requirements, the trigger efficiency is nearly 100%.

Since chargino decay products carry a small amount of energy, the following selection criteria are applied: no significant energy deposit in the low angle calorimeters covering $1.7° \leq \theta \leq 9°$; less than 16 GeV in the hadronic calorimeter; less than 3 GeV in the electromagnetic calorimeter between BGO barrel and endcaps; no muon track with a momentum greater than 10 GeV. Excluding the photon, the remaining energy in the BGO must be less than 16 GeV, and the total calorimetric energy must be less than 18 GeV. High multiplicity events are rejected by requiring less than 10 tracks and less than 15 BGO energy clusters.

After these cuts, 43 data events are selected for 10.8 expected from Standard Model processes which have been simulated. Some of the remaining data events are not compatible with any signals and they are probably due to photon-photon interactions. This is illustrated in Figure 2, which shows the transverse energy imbalance (E_{Tvis}/E_{vis}) distribution for the data, the simulated Standard Model background and the signal (all masses and ΔM folded in the same distribution). It is clear from this distribution that data events with small transverse energy imbalance are not consistent with any signal. Hence, we add the requirement that the transverse energy imbalance must be greater than 0.1.

The photon-photon interaction background should be completely eliminated by the requirement of equation (1). In fact, this is true only for an absolutely hermetic detector, such that deflected electrons are not missed. To investigate this problem a sample of simulated

$e^+e^- \to e^+e^-q\bar{q}\gamma(\gamma)$ events, generated with PHOJET [13] for a mass of the $\gamma\gamma$ system greater than 3 GeV, is used. The expected background from this source, concentrated at low values of transverse energy imbalance, is 0.8 events. This result is not conclusive because masses of the $\gamma\gamma$ system below 3 GeV can not be simulated due to the aforementioned uncertainties on the photon-photon interaction cross section. Nevertheless, it shows that a non-zero background from photon-photon interaction is expected, due to small residual inefficiencies to tag electrons at low angles ($\theta_d < 10°$), which might explain the excess of data.

Finally, 29 data events are selected and 10.7 are expected from the simulated Standard Model background (4.2 from $\mu^+\mu^-\gamma(\gamma)$, 5.5 from $\tau^+\tau^-\gamma(\gamma)$, < 0.06 from $e^+e^-\gamma(\gamma)$, 0.8 from $\nu\bar{\nu}\gamma(\gamma)$, 0.2 from $W^+W^-\gamma(\gamma)$).

4.2 Selections

Three different selections are devised according to the ΔM range explored: low ΔM, very low ΔM and ultra low ΔM selections.

The low ΔM selection is optimized for ΔM around 3 GeV. At such ΔM, charginos decay promptly and their decay products carry enough energy to reach the BGO. This selection requires that the event contains at least 2 tracks with a DCA smaller than 1 cm and a second energy deposit in the BGO.

The very low ΔM selection is optimized for ΔM around 1 GeV whereas the ultra low ΔM selection is optimized for ΔM around 300 MeV and less. At such small ΔM, no muons are able to reach the muon chamber. Therefore, events must not contain muon tracks. The other requirements on the calorimetric energy are modified according to the smaller energy deposited by the chargino decay products. No requirements on the track momentum are applied in the ultra low ΔM selection to take into account the possible high momentum tracks produced by long lived charginos. Table 1 lists all selection cuts for all ΔM regions.

		Selection		
Cut		low ΔM	very low ΔM	ultra low ΔM
hadronic calorimeter energy	$<$	12 GeV	10 GeV	10 GeV
$E_{BGO} - E_\gamma$	$<$	10 GeV	6 GeV	1 GeV
remaining calorimetric energy	$<$	12 GeV	8 GeV	6 GeV
muon momentum	$<$	8 GeV	No muon	No muon
P_t track	$<$	10 GeV	4 GeV	none
transverse energy imbalance	$>$	0.1	0.2	0.3
longitudinal energy imbalance	$<$	0.85	none	none
number of tracks	$<$	10	7	5
number of BGO energy clusters	$<$	15	10	6
isolation angle of the photon	$<$	160°	none	none

Table 1: Requirements for all selections.

The number of selected data events and expected backgrounds are shown in Table 2. This table displays also the number of events selected by the three selections combined. Finally, for a given $\tilde{\chi}_1^\pm$ mass, events are considered as candidates only if the effective centre-of-mass energy is high enough, i.e. the photon recoil mass is greater than twice the $\tilde{\chi}_1^\pm$ mass.

	Selection			
	low ΔM	very low ΔM	ultra low ΔM	Combined
$\mu^+\mu^-\gamma(\gamma)$	0.41	0.08	0.63	0.94
$\tau^+\tau^-\gamma(\gamma)$	1.34	0.39	0.08	1.44
$\nu\bar{\nu}\gamma(\gamma)$	0.54	0.57	0.20	0.64
$W^+W^-\gamma(\gamma)$	0.03	0.01	0.	0.03
Total	2.32	1.05	0.91	3.05
Data	6	1	1	8

Table 2: Number of selected data events and expected from simulated Standard Model backgrounds. The last column displays the same numbers for the three selections combined.

5 Results

The selection efficiency for short-lived charginos with a photon within fiducial cuts is about 35% for $\Delta M \geq 200$ MeV. In Figure 3a the selection efficiency is shown as a function of the chargino decay length. For decay lengths of tens of centimetres the efficiency decreases to approximately 20%, because in that range highly ionising chargino tracks reach the tracking chamber and the BGO calorimeter. The efficiency drops for decay lengths of a few metres. This drop is due to long-lived charginos which produce high momentum tracks in the muon chambers and events without missing energy. This kind of signal, which suffers from the $\mu^+\mu^-\gamma(\gamma)$ background, is taken into account by the search for stable heavy charged particles [14].

In Figure 3b is shown the selection efficiency as a function of ΔM for several values of the chargino decay length. The drop for $\Delta M < 100$ MeV is due to the magnetic field which bends low momentum tracks, such that they do not reach the tracking chamber. This is a major experimental limitation in the search of short-lived charginos for $\Delta M < 50$ MeV. In particular, for $\tilde{\nu}_e$ or $\tilde{e}$ mass degenerate with charginos the decay length is extremely short as long as ΔM is above the electron mass.

In Figure 4a is shown the acceptance for events with an ISR photon within fiducial cuts as a function of the chargino mass. This acceptance also depends on the chargino mixture and on the $\tilde{\nu}$ mass. The total efficiency, product of the efficiency in Figure 3 and the acceptance in Figure 4a, is derived as shown in Figure 4b for a gaugino-like $\tilde{\chi}_1^\pm$. In the same way, efficiencies are also estimated for a higgsino-like $\tilde{\chi}_1^\pm$, and for a gaugino-like $\tilde{\chi}_1^\pm$ in the light $\tilde{\nu}$ case. The evolution of the efficiency with $M_{\tilde{\chi}_1^\pm}$ is essentially governed by the ISR spectrum.

A Standard Model process with a similar signature to the one we search in this analysis is $\nu\bar{\nu}\gamma(\gamma)$. The analysis of $\nu\bar{\nu}\gamma(\gamma)$ events has already been performed on 189 GeV data [15], resulting in a good agreement between observation and Standard Model expectation. Systematic uncertainties affecting the photon identification, which are smaller than 1%, are relevant for the systematics on the efficiency shown in Figure 4b. The loose requirements on the soft charged tracks induce negligible systematics. Larger uncertainties are due to Monte Carlo statistical errors. They range between 6% and 7% according to the chargino mixture and decay length. These systematics are neglected hereafter since the derived limits are already conservative due to the omission of the photon-photon interaction processes, resulting in an underestimation of the background.

Overall we select 8 data events for 3.1 expected from the simulated Standard Model pro-

cesses. We use the signal efficiency, the background prediction and the number of selected events, to derive a 95% confidence level upper limit on the chargino pair-production cross section as a function of ΔM and $M_{\tilde{\chi}_1^\pm}$ as shown in Figure 5. Those limits are obtained by combining the three selections, according to the method in Ref. [16] modified to include the background subtraction.

6 Interpretations in the MSSM

In the MSSM, chargino and neutralino masses depend on 4 parameters: M_1 the U(1) gaugino mass, M_2 the SU(2) gaugino mass, μ the Higgs mixing parameter and $\tan\beta$ the ratio of the two Higgs vacuum expectation values.

Generally, equal gaugino masses at the GUT scale are assumed, such that M_1 and M_2 are not independent parameters. In this case, low ΔM values are possible only if $|\mu| \ll M_2$ and for M_2 values larger than a few TeV. However, models with gaugino mass non-universality can be considered [17] and as mentioned in Ref. [4] low ΔM regions become more natural in these models [18].

Once the unification relation is relaxed, three main regions can lead to low ΔM: $|\mu| \gg M_2$; in this region the $\tilde{\chi}_1^\pm$ mass is almost equal to M_2, $\tilde{\chi}_1^\pm$ and $\tilde{\chi}_1^0$ are both gaugino-like and ΔM can be small if $M_1 \gtrsim M_2$. $|\mu| \ll M_2$; in this region $\tilde{\chi}_1^0$ and $\tilde{\chi}_1^\pm$ are both higgsino-like and nearly mass degenerate, independently of the values of M_1 and M_2. Their masses are almost equal to $|\mu|$. $M_1 \gtrsim 4M_2$; in this region of the parameter space $\tilde{\chi}_1^0$ and $\tilde{\chi}_1^\pm$ mass degeneracy can be obtained for pure or mixed $\tilde{\chi}_1^\pm$ states.

We derive chargino mass limits as a function of ΔM for all these scenarios. The limits are shown in Figures 6 and 7. For ΔM between 300 MeV and 1 GeV, gaugino-like $\tilde{\chi}_1^\pm$ are excluded up to 83.5 GeV if the $\tilde{\nu}$ is heavy (Figure 6a) and up to 58.8 GeV for any $\tilde{\nu}$ mass (Figure 7a), where cross sections smaller by an order of magnitude are predicted. In Figure 7a the limit is shown as a function of $M_{\tilde{\chi}_1^\pm} - M_{\rm inv}$, where the invisible particle can be either the lightest neutralino or the scalar neutrino. For the same ΔM range, higgsino-like $\tilde{\chi}_1^\pm$ are excluded up to 80.0 GeV (Figure 6b).

The results of this search are combined with the results of the standard $\tilde{\chi}_1^\pm$ search [2] and of the stable heavy charged particles search [14] as shown in Figures 6 and 7. The search with an ISR photon fills the gap between the two previous analyses and allows to derive direct search $\tilde{\chi}_1^\pm$ mass limits independent of ΔM.

The intersection between the ISR search and the stable heavy charged particles search occurs for decay lengths of order 10 cm. However, the relation between the chargino decay length and the ΔM is dependent on the supersymmetric parameters. Due to the mild dependence of the efficiency on ΔM, a scan on the MSSM parameters is done to check the size of the overlap between these two searches. The relation between the decay length and ΔM used to derive the limits shown in Figures 6a, 6b and 7a, is always the most conservative independently of the choice for the chargino mixture used for the cross section calculation. On the contrary, in Figure 7b, where the Constrained MSSM [19] is used, chargino and neutralino mixtures are uniquely defined and used both for the decay length and cross section calculations.

Assuming that scalar particles are sufficiently heavy to be able to neglect their contributions in chargino production and decay, the following chargino mass limits are derived at 95% C.L.:

$$M_{\tilde{\chi}_1^\pm} > 78.9 \text{ GeV} \quad \text{gaugino-like charginos}$$
$$M_{\tilde{\chi}_1^\pm} > 69.4 \text{ GeV} \quad \text{higgsino-like charginos.}$$

As mentioned in Section 3, the chargino decay length also depends on the masses of the scalar particles. For light scalar quarks, hadronic decays are enhanced and a sharp change from short to long-lived charginos is expected for ΔM around the pion mass. In this case, the chargino mass limit is 0.5 GeV lower for gaugino-like $\tilde{\chi}_1^{\pm}$, while it is unchanged for higgsino-like $\tilde{\chi}_1^{\pm}$. In the case of light scalar taus or $\tilde{\nu}_\tau$, the chargino mass limit is unchanged for gaugino-like $\tilde{\chi}_1^{\pm}$ and lowered by 0.8 GeV for higgsino-like $\tilde{\chi}_1^{\pm}$. For light scalar muons or $\tilde{\nu}_\mu$ the chargino mass limit is lowered by 1.3 GeV for gaugino-like $\tilde{\chi}_1^{\pm}$, while it is unchanged for higgsino-like $\tilde{\chi}_1^{\pm}$.

No direct search mass limits are derived for light $\tilde{\nu}_{\mathrm{e}}$ or $\tilde{\mathrm{e}}$ masses, because there is still an uncovered ΔM region between the stable heavy charged particles search and the search with an ISR photon. This gap is due to the shorter $\tilde{\chi}_1^{\pm}$ decay length when these scalar particles are mass degenerate with or lighter than the chargino. In such a case, charginos are stable only for ΔM below the electron mass.

Figure 7b shows the exclusion in the Constrained MSSM [19] in the higgsino region (very large M_2 values). The exclusion from the standard search is obtained by combining the contribution of the $\mathrm{e^+e^-} \to \tilde{\chi}_2^0\tilde{\chi}_1^0$ process [2] with the chargino pair production:

$$\mathrm{M}_{\tilde{\chi}_1^{\pm}} > 76.8 \text{ GeV} \quad \text{Constrained MSSM.}$$

In the Constrained MSSM, by using the scalar lepton search [20], a limit on the $\tilde{\chi}_1^{\pm}$ mass of 67.7 GeV is also derived in the light $\tilde{\nu}$ case, assuming no mixing in the scalar tau sector. This limit of 67.7 GeV is an absolute lower limit for the chargino in the Constrained MSSM parameter space, since the very large M_2 domain is now excluded by this search.

Acknowledgments

We express our gratitude to the CERN accelerator divisions for the excellent performance of the LEP machine. We also acknowledge and appreciate the effort of the engineers, technicians and support staff who have participated in the construction and maintenance of this experiment.

Author List

The L3 Collaboration:

M.Acciarri,[26] P.Achard,[19] O.Adriani,[16] M.Aguilar-Benitez,[25] J.Alcaraz,[25] G.Alemanni,[22] J.Allaby,[17] A.Aloisio,[28] M.G.Alviggi,[28] G.Ambrosi,[19] H.Anderhub,[48] V.P.Andreev,[6,36] T.Angelescu,[12] F.Anselmo,[9] A.Arefiev,[27] T.Azemoon,[3] T.Aziz,[10] P.Bagnaia,[35] L.Baksay,[43] A.Balandras,[4] R.C.Ball,[3] S.Banerjee,[10] Sw.Banerjee,[10] A.Barczyk,[48,46] R.Barillère,[17] L.Barone,[35] P.Bartalini,[22] M.Basile,[9] R.Battiston,[32] A.Bay,[22] F.Becattini,[16] U.Becker,[14] F.Behner,[48] L.Bellucci,[16] J.Berdugo,[25] P.Berges,[14] B.Bertucci,[32] B.L.Betev,[48] S.Bhattacharya,[10] M.Biasini,[32] A.Biland,[48] J.J.Blaising,[4] S.C.Blyth,[33] G.J.Bobbink,[2] A.Böhm,[1] L.Boldizsar,[13] B.Borgia,[35] D.Bourilkov,[48] M.Bourquin,[19] S.Braccini,[19] J.G.Branson,[39] V.Brigljevic,[48] F.Brochu,[4] A.Buffini,[16] A.Buijs,[44] J.D.Burger,[14] W.J.Burger,[32] A.Button,[3] X.D.Cai,[14] M.Campanelli,[48] M.Capell,[14] G.Cara Romeo,[9] G.Carlino,[28] A.M.Cartacci,[16] J.Casaus,[25] G.Castellini,[16] F.Cavallari,[35] N.Cavallo,[37] C.Cecchi,[32] M.Cerrada,[25] F.Cesaroni,[23] M.Chamizo,[19] Y.H.Chang,[50] U.K.Chaturvedi,[18] M.Chemarin,[24] A.Chen,[50] G.Chen,[7] G.M.Chen,[7] H.F.Chen,[20] H.S.Chen,[7] G.Chiefari,[28] L.Cifarelli,[38] F.Cindolo,[9] C.Civinini,[16] I.Clare,[14] R.Clare,[14] G.Coignet,[4] A.P.Colijn,[2] N.Colino,[25] S.Costantini,[5] F.Cotorobai,[12] B.Cozzoni,[9] B.de la Cruz,[25] A.Csilling,[13] S.Cucciarelli,[32] T.S.Dai,[14] J.A.van Dalen,[30] R.D'Alessandro,[16] R.de Asmundis,[28] P.Déglon,[19] A.Degré,[4] K.Deiters,[46] D.della Volpe,[28] P.Denes,[34] F.DeNotaristefani,[35] A.De Salvo,[48] M.Diemoz,[35] D.van Dierendonck,[2] F.Di Lodovico,[48] C.Dionisi,[35] M.Dittmar,[48] A.Dominguez,[39] A.Doria,[28] M.T.Dova,[18,♯] D.Duchesneau,[4] D.Dufournaud,[4] P.Duinker,[2] I.Duran,[40] H.El Mamouni,[24] A.Engler,[33] F.J.Eppling,[14] F.C.Erné,[2] P.Extermann,[19] M.Fabre,[46] R.Faccini,[35] M.A.Falagan,[25] S.Falciano,[35,17] A.Favara,[17] J.Fay,[24] O.Fedin,[36] M.Felcini,[48] T.Ferguson,[33] F.Ferroni,[35] H.Fesefeldt,[1] E.Fiandrini,[32] J.H.Field,[19] F.Filthaut,[17] P.H.Fisher,[14] I.Fisk,[39] G.Forconi,[14] L.Fredj,[19] K.Freudenreich,[48] C.Furetta,[26] Yu.Galaktionov,[27,14] S.N.Ganguli,[10] P.Garcia-Abia,[5] M.Gataullin,[31] S.S.Gau,[11] S.Gentile,[35,17] N.Gheordanescu,[12] S.Giagu,[35] Z.F.Gong,[20] G.Grenier,[24] O.Grimm,[48] M.W.Gruenewald,[8] M.Guida,[38] R.van Gulik,[2] V.K.Gupta,[34] A.Gurtu,[10] L.J.Gutay,[45] D.Haas,[5] A.Hasan,[29] D.Hatzifotiadou,[9] T.Hebbeker,[8] A.Hervé,[17] P.Hidas,[13] J.Hirschfelder,[33] H.Hofer,[48] G. Holzner,[48] H.Hoorani,[33] S.R.Hou,[50] I.Iashvili,[47] B.N.Jin,[7] L.W.Jones,[3] P.de Jong,[2] I.Josa-Mutuberría,[25] R.A.Khan,[18] M.Kaur,[18,◇] M.N.Kienzle-Focacci,[19] D.Kim,[35] D.H.Kim,[42] J.K.Kim,[42] S.C.Kim,[42] J.Kirkby,[17] D.Kiss,[13] W.Kittel,[30] A.Klimentov,[14,27] A.C.König,[30] A.Kopp,[47] V.Koutsenko,[14,27] M.Kräber,[48] R.W.Kraemer,[33] W.Krenz,[1] A.Krüger,[47] A.Kunin,[14,27] P.Ladron de Guevara,[25] I.Laktineh,[24] G.Landi,[16] K.Lassila-Perini,[48] M.Lebeau,[17] A.Lebedev,[14] P.Lebrun,[24] P.Lecomte,[48] P.Lecoq,[17] P.Le Coultre,[48] H.J.Lee,[8] J.M.Le Goff,[17] R.Leiste,[47] E.Leonardi,[35] P.Levtchenko,[36] C.Li,[20] S.Likhoded,[47] C.H.Lin,[50] W.T.Lin,[50] F.L.Linde,[2] L.Lista,[28] Z.A.Liu,[7] W.Lohmann,[47] E.Longo,[35] Y.S.Lu,[7] K.Lübelsmeyer,[1] C.Luci,[17,35] D.Luckey,[14] L.Lugnier,[24] L.Luminari,[35] W.Lustermann,[48] W.G.Ma,[20] M.Maity,[10] L.Malgeri,[17] A.Malinin,[17] C.Maña,[25] D.Mangeol,[30] P.Marchesini,[48] G.Marian,[15] J.P.Martin,[24] F.Marzano,[35] G.G.G.Massaro,[2] K.Mazumdar,[10] R.R.McNeil,[6] S.Mele,[17] L.Merola,[28] M.Meschini,[16] W.J.Metzger,[30] M.von der Mey,[1] A.Mihul,[12] H.Milcent,[17] G.Mirabelli,[35] J.Mnich,[17] G.B.Mohanty,[10] P.Molnar,[8] B.Monteleoni,[16,†] T.Moulik,[10] G.S.Muanza,[24] F.Muheim,[19] A.J.M.Muijs,[2] M.Musy,[35] M.Napolitano,[28] F.Nessi-Tedaldi,[48] H.Newman,[31] T.Niessen,[1] A.Nisati,[35] H.Nowak,[47] Y.D.Oh,[42] G.Organtini,[35] A.Oulianov,[27] C.Palomares,[25] D.Pandoulas,[1] S.Paoletti,[35,17] P.Paolucci,[28] R.Paramatti,[35] H.K.Park,[33] I.H.Park,[42] G.Pascale,[35] G.Passaleva,[17] S.Patricelli,[28] T.Paul,[11] M.Pauluzzi,[32] C.Paus,[17] F.Pauss,[48] M.Pedace,[35] S.Pensotti,[26] D.Perret-Gallix,[4] B.Petersen,[30] D.Piccolo,[28] F.Pierella,[9] M.Pieri,[16] P.A.Piroué,[34] E.Pistolesi,[26] V.Plyaskin,[27] M.Pohl,[19] V.Pojidaev,[27,16] H.Postema,[14] J.Pothier,[17] N.Produit,[19] D.O.Prokofiev,[45] D.Prokofiev,[36] J.Quartieri,[38] G.Rahal-Callot,[48,17] M.A.Rahaman,[10] P.Raics,[15] N.Raja,[10] R.Ramelli,[48] P.G.Rancoita,[26] A.Raspereza,[47] G.Raven,[39] P.Razis,[29] D.Ren,[48] M.Rescigno,[35] S.Reucroft,[11] T.van Rhee,[44] S.Riemann,[47] K.Riles,[3] A.Robohm,[48] J.Rodin,[43] B.P.Roe,[3] L.Romero,[25] A.Rosca,[8] S.Rosier-Lees,[4] J.A.Rubio,[17] D.Ruschmeier,[8] H.Rykaczewski,[48] S.Saremi,[6] S.Sarkar,[35] J.Salicio,[17] E.Sanchez,[17] M.P.Sanders,[30] M.E.Sarakinos,[21] C.Schäfer,[17] V.Schegelsky,[36] S.Schmidt-Kaerst,[1] D.Schmitz,[1] H.Schopper,[49] D.J.Schotanus,[30] G.Schwering,[1] C.Sciacca,[28] D.Sciarrino,[19] A.Seganti,[9] L.Servoli,[32] S.Shevchenko,[31] N.Shivarov,[41] V.Shoutko,[27] E.Shumilov,[27] A.Shvorob,[31] T.Siedenburg,[1] D.Son,[42] B.Smith,[33] P.Spillantini,[16] M.Steuer,[14] D.P.Stickland,[34] A.Stone,[6] H.Stone,[34,†] B.Stoyanov,[41] A.Straessner,[1] K.Sudhakar,[10] G.Sultanov,[18] L.Z.Sun,[20] H.Suter,[48] J.D.Swain,[18] Z.Szillasi,[43,¶] T.Sztaricskai,[43,¶] X.W.Tang,[7] L.Tauscher,[5] L.Taylor,[11] B.Tellili,[24] C.Timmermans,[30] Samuel C.C.Ting,[14] S.M.Ting,[14] S.C.Tonwar,[10] J.Tóth,[13] C.Tully,[17] K.L.Tung,[7] Y.Uchida,[14] J.Ulbricht,[48] E.Valente,[35] G.Vesztergombi,[13] I.Vetlitsky,[27] D.Vicinanza,[38] G.Viertel,[48] S.Villa,[11] M.Vivargent,[4] S.Vlachos,[5] I.Vodopianov,[36] H.Vogel,[33] H.Vogt,[47] I.Vorobiev,[27] A.A.Vorobyov,[36] A.Vorvolakos,[29] M.Wadhwa,[5] W.Wallraff,[1] M.Wang,[14] X.L.Wang,[20] Z.M.Wang,[20] A.Weber,[1] M.Weber,[1] P.Wienemann,[1] H.Wilkens,[30] S.X.Wu,[14] S.Wynhoff,[17] L.Xia,[31] Z.Z.Xu,[20] B.Z.Yang,[20] C.G.Yang,[7] H.J.Yang,[7] M.Yang,[7] J.B.Ye,[20] S.C.Yeh,[51] An.Zalite,[36] Yu.Zalite,[36] Z.P.Zhang,[20] G.Y.Zhu,[7] R.Y.Zhu,[31] A.Zichichi,[9,17,18] G.Zilizi,[43,¶] M.Zöller.[1]

1 I. Physikalisches Institut, RWTH, D-52056 Aachen, FRG[§]
III. Physikalisches Institut, RWTH, D-52056 Aachen, FRG[§]
2 National Institute for High Energy Physics, NIKHEF, and University of Amsterdam, NL-1009 DB Amsterdam, The Netherlands
3 University of Michigan, Ann Arbor, MI 48109, USA
4 Laboratoire d'Annecy-le-Vieux de Physique des Particules, LAPP,IN2P3-CNRS, BP 110, F-74941 Annecy-le-Vieux CEDEX, France
5 Institute of Physics, University of Basel, CH-4056 Basel, Switzerland
6 Louisiana State University, Baton Rouge, LA 70803, USA
7 Institute of High Energy Physics, IHEP, 100039 Beijing, China[△]
8 Humboldt University, D-10099 Berlin, FRG[§]
9 University of Bologna and INFN-Sezione di Bologna, I-40126 Bologna, Italy
10 Tata Institute of Fundamental Research, Bombay 400 005, India
11 Northeastern University, Boston, MA 02115, USA
12 Institute of Atomic Physics and University of Bucharest, R-76900 Bucharest, Romania
13 Central Research Institute for Physics of the Hungarian Academy of Sciences, H-1525 Budapest 114, Hungary[‡]
14 Massachusetts Institute of Technology, Cambridge, MA 02139, USA
15 KLTE-ATOMKI, H-4010 Debrecen, Hungary[¶]
16 INFN Sezione di Firenze and University of Florence, I-50125 Florence, Italy
17 European Laboratory for Particle Physics, CERN, CH-1211 Geneva 23, Switzerland
18 World Laboratory, FBLJA Project, CH-1211 Geneva 23, Switzerland
19 University of Geneva, CH-1211 Geneva 4, Switzerland
20 Chinese University of Science and Technology, USTC, Hefei, Anhui 230 029, China[△]
21 SEFT, Research Institute for High Energy Physics, P.O. Box 9, SF-00014 Helsinki, Finland
22 University of Lausanne, CH-1015 Lausanne, Switzerland
23 INFN-Sezione di Lecce and Universitá Degli Studi di Lecce, I-73100 Lecce, Italy
24 Institut de Physique Nucléaire de Lyon, IN2P3-CNRS,Université Claude Bernard, F-69622 Villeurbanne, France
25 Centro de Investigaciones Energéticas, Medioambientales y Tecnologícas, CIEMAT, E-28040 Madrid, Spain[♭]
26 INFN-Sezione di Milano, I-20133 Milan, Italy
27 Institute of Theoretical and Experimental Physics, ITEP, Moscow, Russia
28 INFN-Sezione di Napoli and University of Naples, I-80125 Naples, Italy
29 Department of Natural Sciences, University of Cyprus, Nicosia, Cyprus
30 University of Nijmegen and NIKHEF, NL-6525 ED Nijmegen, The Netherlands
31 California Institute of Technology, Pasadena, CA 91125, USA
32 INFN-Sezione di Perugia and Universitá Degli Studi di Perugia, I-06100 Perugia, Italy
33 Carnegie Mellon University, Pittsburgh, PA 15213, USA
34 Princeton University, Princeton, NJ 08544, USA
35 INFN-Sezione di Roma and University of Rome, "La Sapienza", I-00185 Rome, Italy
36 Nuclear Physics Institute, St. Petersburg, Russia
37 INFN-Sezione di Napoli and University of Potenza, I-85100 Potenza, Italy
38 University and INFN, Salerno, I-84100 Salerno, Italy
39 University of California, San Diego, CA 92093, USA
40 Dept. de Fisica de Particulas Elementales, Univ. de Santiago, E-15706 Santiago de Compostela, Spain
41 Bulgarian Academy of Sciences, Central Lab. of Mechatronics and Instrumentation, BU-1113 Sofia, Bulgaria
42 Center for High Energy Physics, Adv. Inst. of Sciences and Technology, 305-701 Taejon, Republic of Korea
43 University of Alabama, Tuscaloosa, AL 35486, USA
44 Utrecht University and NIKHEF, NL-3584 CB Utrecht, The Netherlands
45 Purdue University, West Lafayette, IN 47907, USA
46 Paul Scherrer Institut, PSI, CH-5232 Villigen, Switzerland
47 DESY, D-15738 Zeuthen, FRG
48 Eidgenössische Technische Hochschule, ETH Zürich, CH-8093 Zürich, Switzerland
49 University of Hamburg, D-22761 Hamburg, FRG
50 National Central University, Chung-Li, Taiwan, China
51 Department of Physics, National Tsing Hua University, Taiwan, China
§ Supported by the German Bundesministerium für Bildung, Wissenschaft, Forschung und Technologie
‡ Supported by the Hungarian OTKA fund under contract numbers T019181, F023259 and T024011.
¶ Also supported by the Hungarian OTKA fund under contract numbers T22238 and T026178.
♭ Supported also by the Comisión Interministerial de Ciencia y Tecnología.
♯ Also supported by CONICET and Universidad Nacional de La Plata, CC 67, 1900 La Plata, Argentina.
♢ Also supported by Panjab University, Chandigarh-160014, India.
△ Supported by the National Natural Science Foundation of China.
† Deceased.

References

[1] H.P. Nilles, Phys. Rep. **110** (1984) 1;
H.E. Haber and G.L. Kane, Phys. Rep. **117** (1985) 75.

[2] L3 Collaboration, M. Acciarri *et al.*, CERN-EP/99-127, accepted by Phys. Lett. B.

[3] K. Riles *et al.*, Phys. Rev. **D 42** (1990) 1.

[4] C.H. Chen, M. Drees and J.F. Gunion, Phys. Rev. Lett. **76** (1996) 2002, Erratum Phys. Rev. Lett. **82** (1999) 3192.

[5] DELPHI Collaboration, P. Abreu et al., Eur. Phys. J. **C 11** (1999) 1–17.

[6] L3 Collaboration, B. Adeva *et al.*, Nucl. Instr. and Meth. **A 289** (1990) 35;
M. Chemarin *et al.*, Nucl. Instr. and Meth. **A 349** (1994) 345;
M. Acciarri *et al.*, Nucl. Instr. and Meth. **A 351** (1994) 300;
G. Basti *et al.*, Nucl. Instr. and Meth. **A 374** (1996) 293;
I.C. Brock *et al.*, Nucl. Instr. and Meth. **A 381** (1996) 236;
A. Adam *et al.*, Nucl. Instr. and Meth. **A 383** (1996) 342.

[7] The `KORALZ` version 4.02 is used.
S. Jadach, B.F.L. Ward and Z. Wąs, Comp. Phys. Comm. **79** (1994) 503.

[8] `KORALW` version 1.33 is used.
M. Skrzypek *et al.*, Comp. Phys. Comm. **94** (1996) 216;
M. Skrzypek *et al.*, Phys. Lett. **B 372** (1996) 289.

[9] The `TEEGG` version 7.1 is used.
D. Karlen, Nucl. Phys. **B 289** (1987) 23.

[10] `SUSYGEN` version 2.2 is used.
S. Katsanevas and P. Morawitz, Comp. Phys. Comm. **112** (1998) 227.

[11] The L3 detector simulation is based on GEANT Version 3.15.
See R. Brun et al., "GEANT 3", CERN DD/EE/84-1 (Revised), September 1987.

[12] The `GHEISHA` program, H. Fesefeldt, RWTH Aachen Report PITHA 85/02 (1985).

[13] `PHOJET` version 1.10 is used.
R. Engel, Z. Phys. C 66 (1995) 203;
R. Engel and J. Ranft, Phys. Rev. D 54 (1996) 4244.

[14] L3 Collaboration, M. Acciarri *et al.*, Phys. Lett. **B 462** (1999) 354.

[15] L3 Collaboration, M. Acciarri *et al.*, CERN-EP/99-129, accepted by Phys. Lett.

[16] J.F. Grivaz and F. Le Diberder, Complementary analyses and acceptance optimization in new particle searches, Preprint Lal 92-37 (June 1992).

[17] G. Anderson *et al.*, in DPF/DPB Summer Study on New Directions for High Energy Physics: Snowmass '96, Snowmass, CO, USA; 25 Jun - 12 Jul 1996, (D.G. Cassel, L. Trindle-Gennari and R.H. Siemann, APS, New York, 1997), p. 669.

[18] C.H. Chen, M. Drees and J.F. Gunion, Phys. Rev. **D 55** (1997) 330, Erratum Phys. Rev. Lett. **82** (1999) 3192.

[19] See for instance:
L. Ibanez, Phys. Lett. **B 118** (1982) 73;
R. Barbieri, S. Farrara and C. Savoy, Phys. Lett. **B 119** (1982) 343.

[20] L3 Collaboration, M. Acciarri *et al.*, CERN-EP/99-128, accepted by Phys. Lett.

[21] C. Caso *et al.*, *Review of Particle Physics*, Eur. Phys. J. **C 3** (1998) 1.

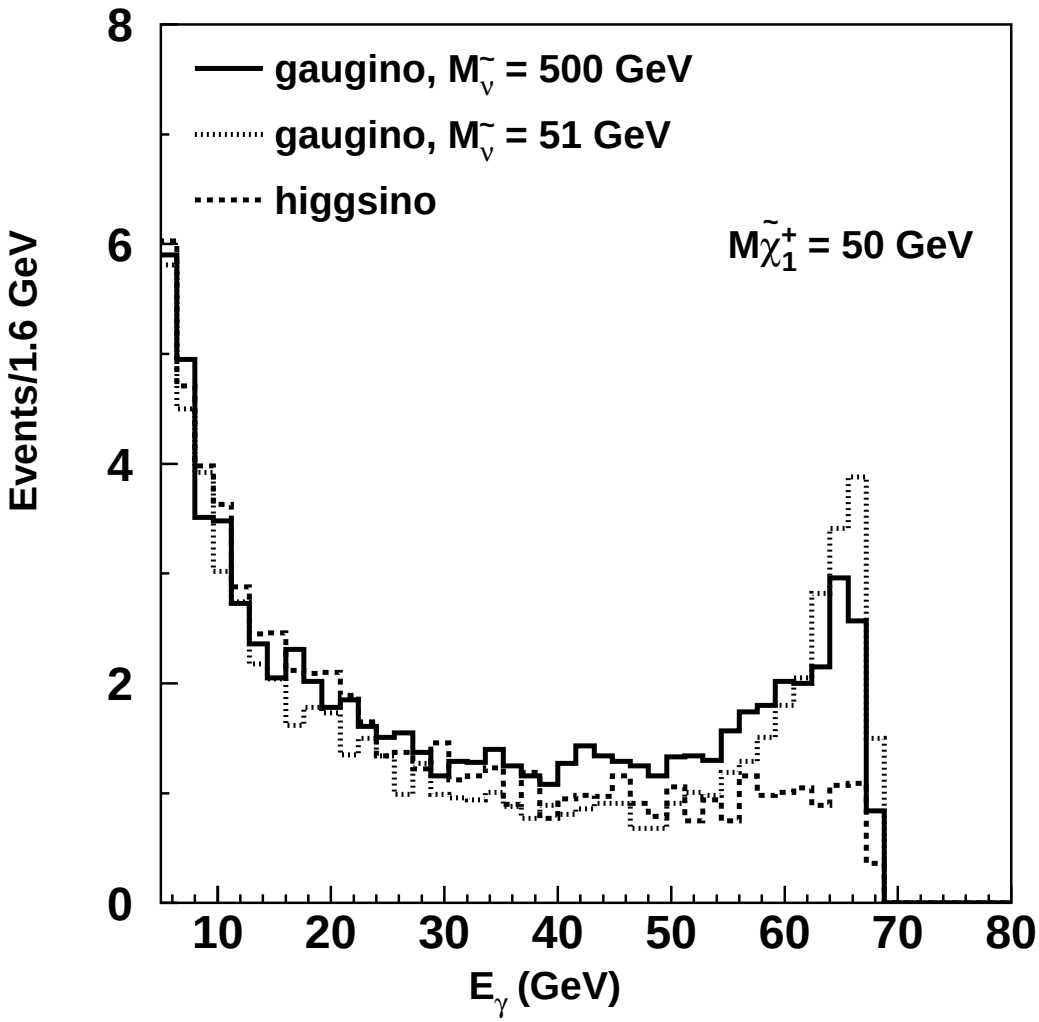

Figure 1: ISR photon energy spectrum for 50 GeV chargino pair production for a photon at least 10° away from the beam pipe. Distributions are shown for gaugino-like chargino with $M_{\tilde{\nu}} = 500$ GeV (solid line) and $M_{\tilde{\nu}} = M_{\tilde{\chi}_1^\pm} + 1$ GeV (dotted line), and for higgsino-like charginos (dashed line) assuming an arbitrary common cross section of about 6 pb.

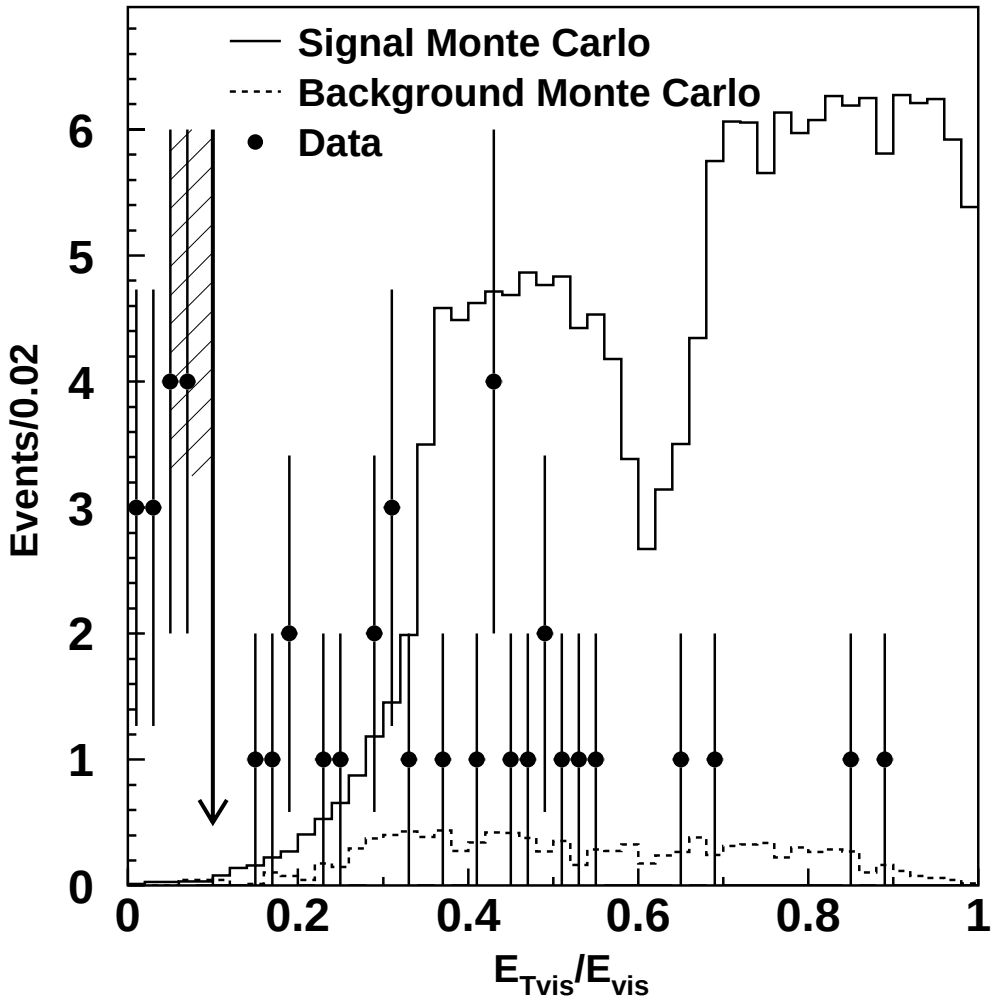

Figure 2: Transverse energy imbalance for the data, the simulated Standard Model background and the signal simulations all masses and ΔM folded in (arbitrary cross section of about 60 pb). The dip around 0.65 in the signal distribution is due to the gap at $\theta \sim 40^\circ$ between BGO barrel and endcaps. The arrow shows the cut position.

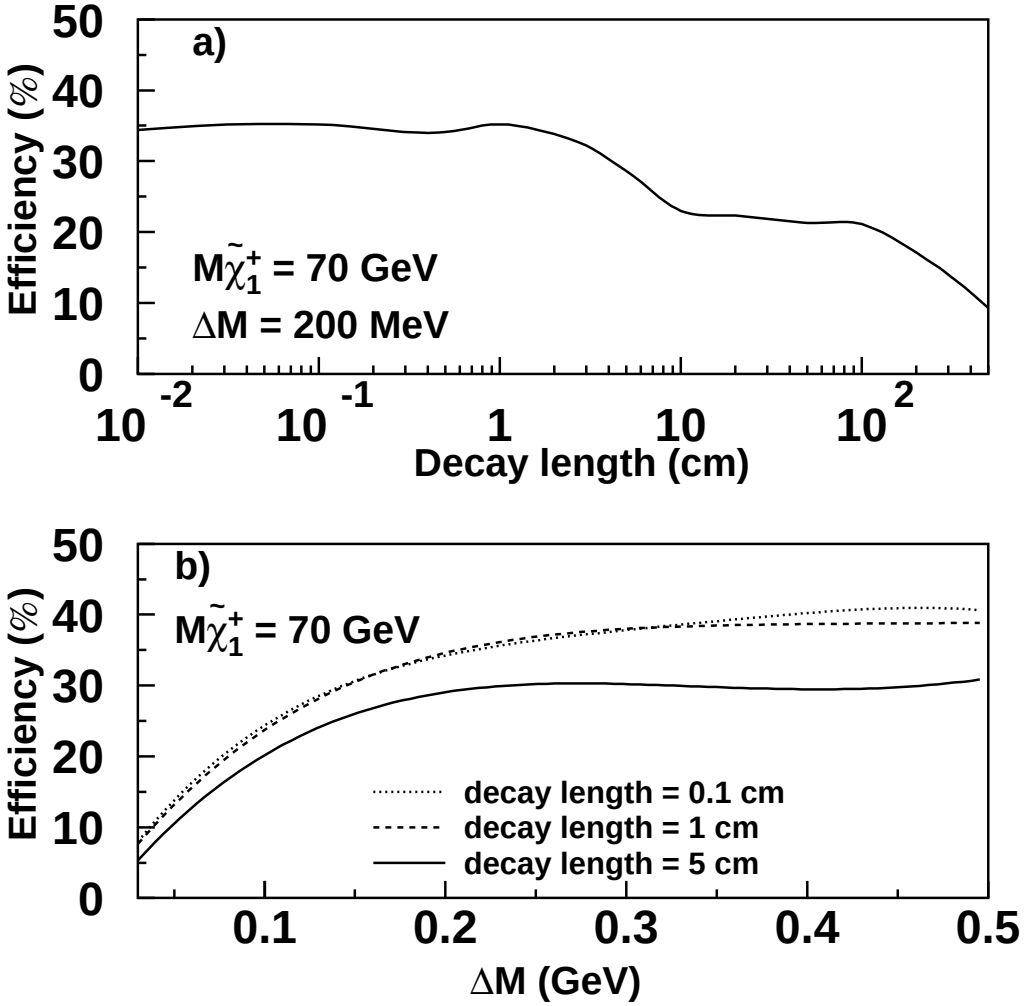

Figure 3: a) Selection efficiency as a function of the chargino decay length for ΔM = 200 MeV. b) Selection efficiency as a function of ΔM for several values of the decay length. Both plots are for a 70 GeV chargino and for an ISR photon within fiducial cuts.

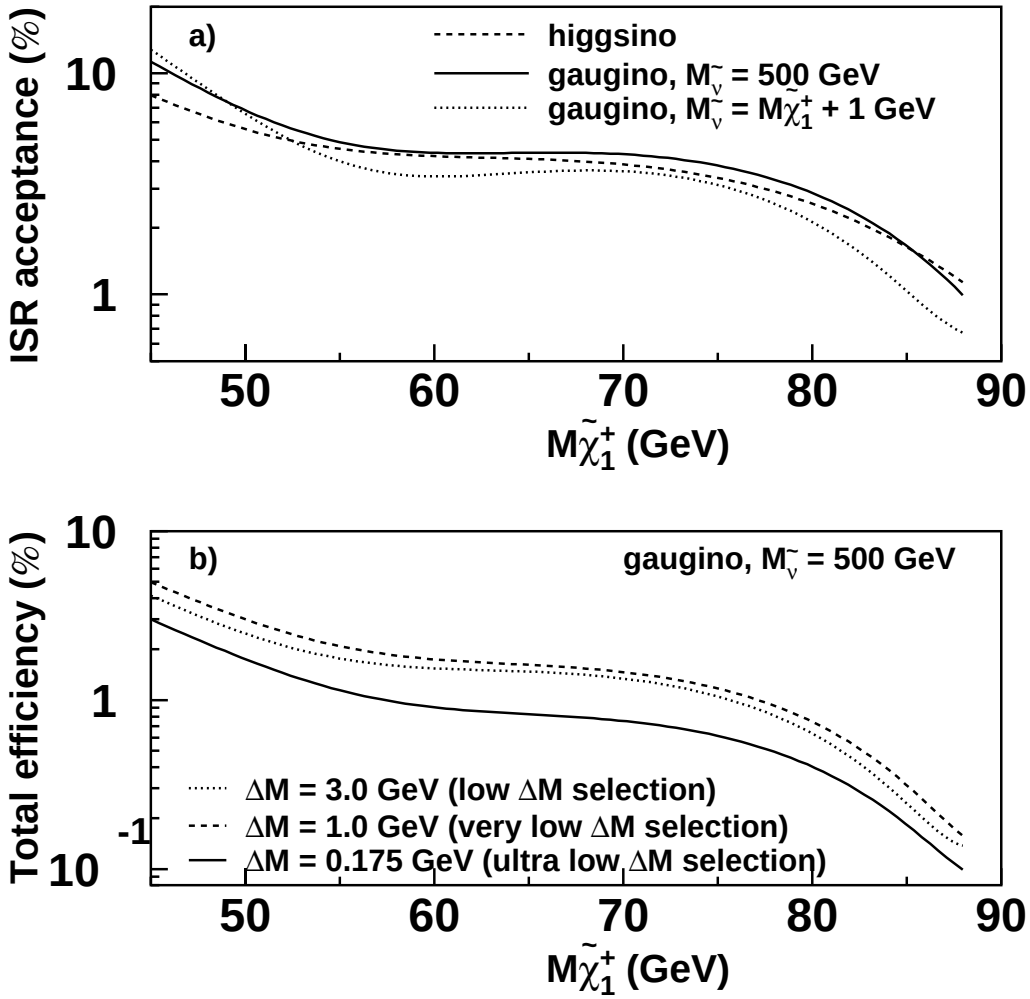

Figure 4: a) Acceptance for events with an ISR photon within fiducial cuts as a function of $M_{\tilde{\chi}_1^\pm}$ for several chargino mixtures and $\tilde{\nu}$ masses. b) Total selection efficiency as a function of $M_{\tilde{\chi}_1^\pm}$ for several ΔM values and in the case of a gaugino-like $\tilde{\chi}_1^\pm$and a heavy $\tilde{\nu}$.

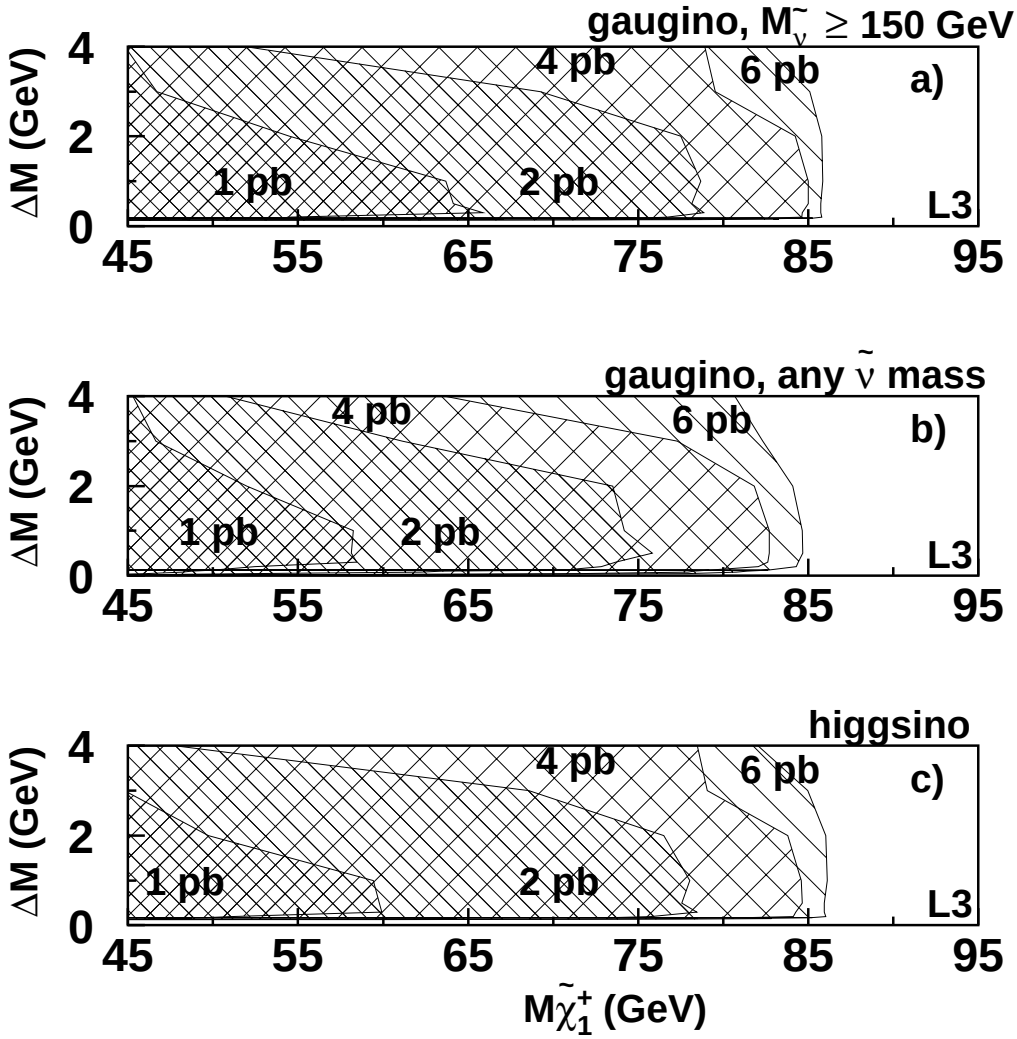

Figure 5: 95% C.L. cross section upper limits as a function of $M_{\tilde{\chi}_1^\pm}$ and ΔM for gaugino-like charginos with a) $M_{\tilde{\nu}} \gtrsim 150$ GeV and b) any $\tilde{\nu}$ mass, and c) for higgsino-like charginos. For these upper limits, for any ΔM the smallest decay length compatible with the MSSM is used.

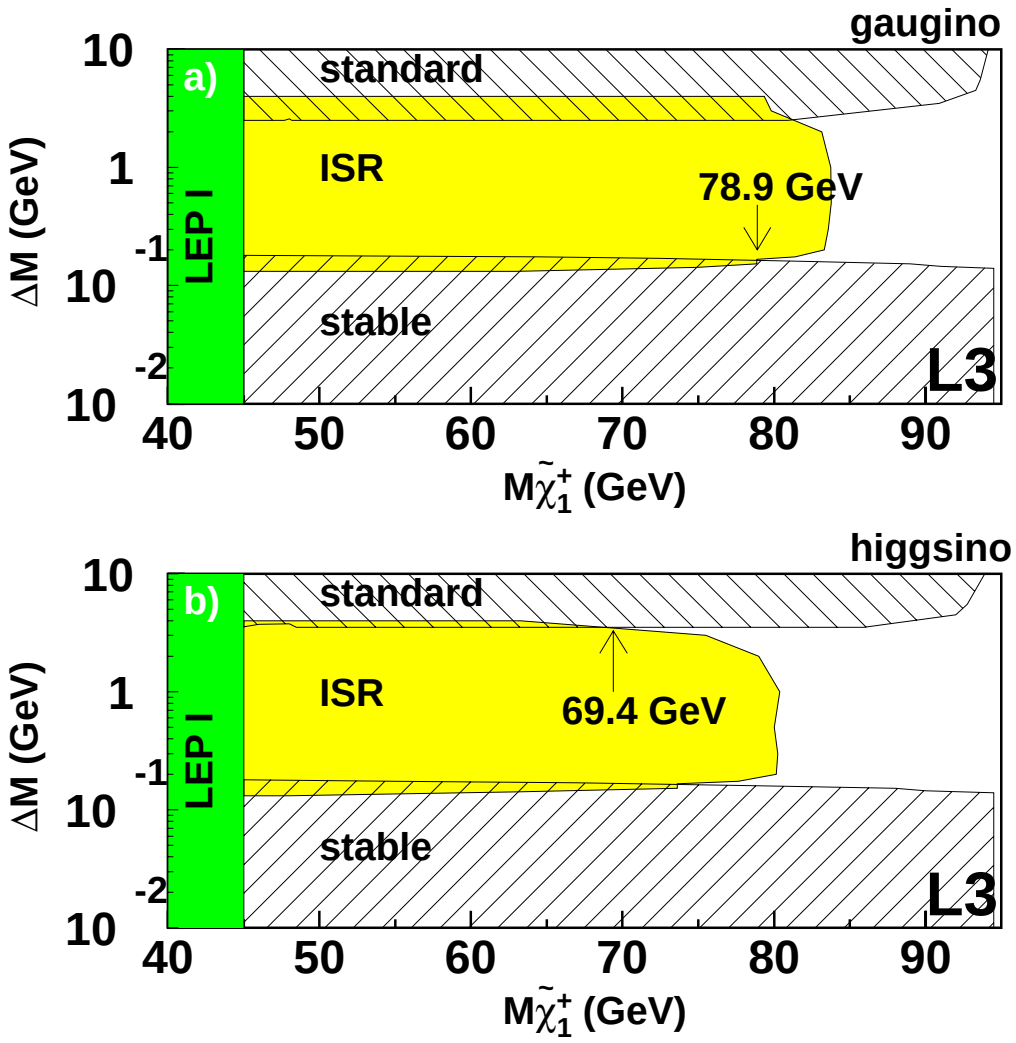

Figure 6: 95% C.L. chargino mass limits as a function of ΔM a) for a gaugino-like $\tilde{\chi}_1^{\pm}$ with a heavy $\tilde{\nu}$ and b) for higgsino-like $\tilde{\chi}_1^{\pm}$. On each plot the top hatched area corresponds to the standard search [2], the bottom hatched area corresponds to the search for heavy stable charged particles [14] and the grey shaded area to this search. The exclusion from LEP1 results on the Z width [21] is also shown.

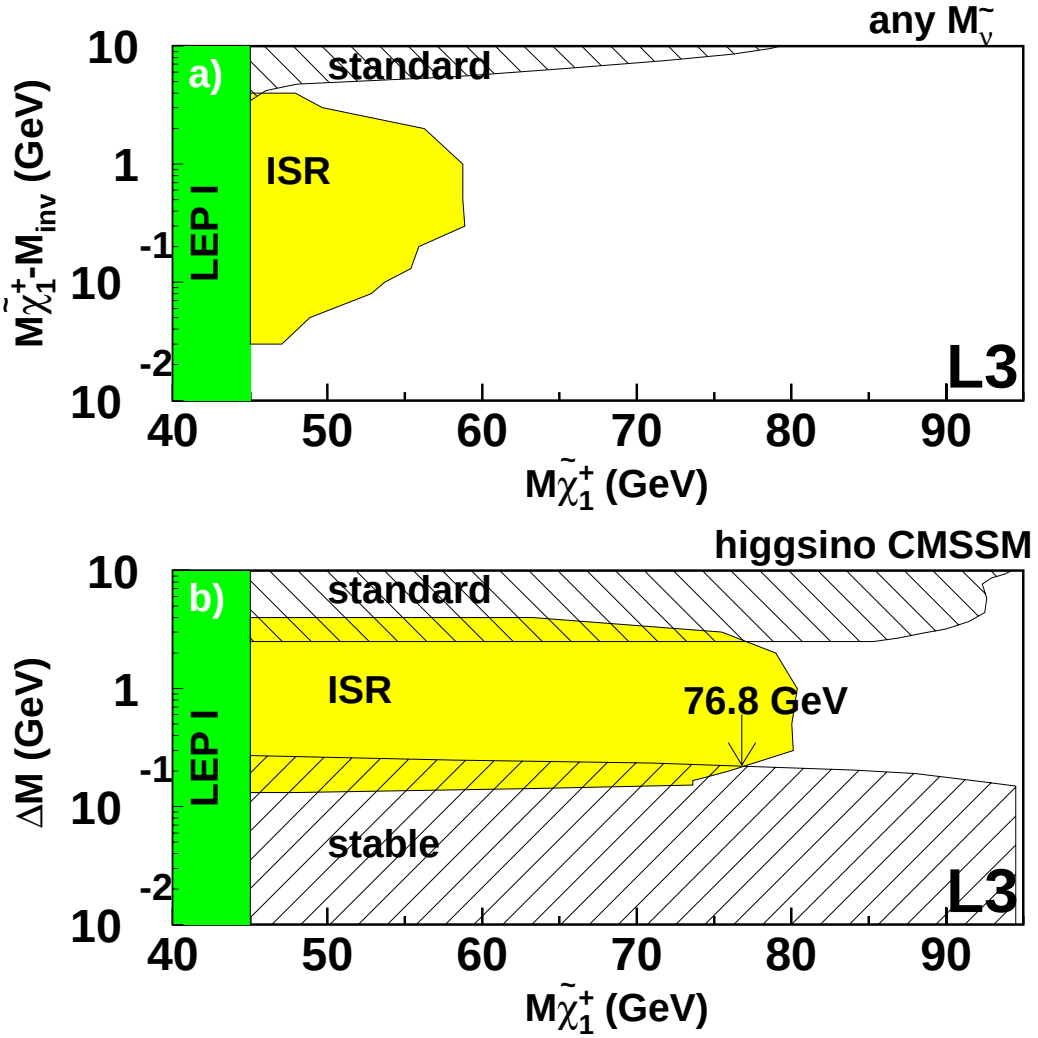

Figure 7: 95% C.L. chargino mass limits a) as a function of $M_{\tilde{\chi}_1^\pm} - M_{inv}$ for a gaugino-like $\tilde{\chi}_1^\pm$ and for any $\tilde{\nu}$ mass and b) as a function of ΔM for a higgsino-like $\tilde{\chi}_1^\pm$ in the Constrained MSSM (CMSSM). On each plot the top hatched area corresponds to the standard search [2], the bottom hatched area corresponds to the search for heavy stable charged particles [14] and the grey shaded area to this search. The exclusion from LEP1 results on the Z width [21] is also shown.